Essential Readings in Light Metals: Aluminum Reduction Technology.
Edited by Geoff Bearne, Marc Dupuis and Gary Tarcy.

MAGNETICS AND METAL PAD INSTABILITY

N. Urata

Kaiser Aluminum & Chemical Corporation
Center for Technology
P. O. Box 877
Pleasanton, CA 94566

A method to evaluate the metal pad instability was developed. The electrolyte and molten metal were treated as a two-layer fluid whose interface is electromagnetically disturbed. An interfacial wave equation with the electromagnetic force term in it was solved along with an equation for the electrical current distribution.

The result showed that the instability was governed by the distribution pattern of the vertical component of the magnetic field rather than its absolute intensity.

Based on the result, an alteration was made to our prototype 200 kA cell bus configuration, which led to an improvement of the metal pad stability.

Introduction

In an aluminum reduction cell, two liquid layers stratify. Molten electrolyte of density around 2.1 g/cm^3 forms the upper layer, and liquid aluminum of density 2.3 g/cm^3 forms the lower layer. The shape of the cell is in most cases rectangular, 3 ∿ 10m long and 2 ∿ 4m wide. The depth of each layer underneath the carbon anode, is 4 ∿ 5 cm and 10 ∿ 40 cm respectively. The anode is placed above the electrolyte layer. A carbon cathode contains the liquids and supports the metal layer. In simplifying this structure in fluid mechanics terms, the aluminum reduction cell consists of two shallow fluid layers confined in a rectangular pool. Under the influence of various forces, it is expected that waves occur on the interface surface of the two layers.

What makes this fluid system unique is an existence of a strong electromagnetic force and its discontinuity across the interface boundary. A large DC current (50 ∿ 200 kA) passes through the system and generates a magnetic field. The flux density reaches 200 ∿ 300 Gauss at its highest location in high current cells. Thus, a major force acting on the liquids is a body force generated by the internal electrical current and the magnetic field.

In this paper three possible waves are investigated, ① a capillary wave, ② a short period wave and ③ a long period wave. A theory for the long period wave developed by the author[1] is summarized and its practical application to a 200 kA cell development is described.

Capillary Wave

The surface tension of the liquid aluminum contacting the molten bath is around β =0.52 Newton/m. So the capillary constant for the surface becomes:

$$a=\sqrt{2\beta/g(\rho_2-\rho_1)} \quad = 0.023 \text{ m} \qquad (1)$$

g: gravitational acceleration (m)
ρ_1, ρ_2 : density of the bath and the metal (kg/m^3)

This length is much smaller than a typical cell dimension, indicating the wave is a ripple on the interface surface, and plays a minor role in the slow fluid motion with a wave length of over 1m.

Short Period Wave

When the anode-cathode separation which characterizes cell operation is extremely small in a localized area or there exists a shorting of the current between the anode and the liquid metal in the small area, we observe a sharp downward spike of the voltage on the continuous cell voltage recording chart. The period of this spike varies from a couple

of seconds to 20 seconds. It appears that the mechanism of this motion is related to the intense localized electrical current. This local current concentration in the molten bath disperses when the current flows into the highly conductive liquid metal. It is known that such a concentrated electrical current generates a circumferential magnetic field which interacts with the current and generates a pinch force.

In the present case a steep gradient of the pinch force is generated due to a sudden change in the current concentration across the interface. This pinch force (divergence of the force) in the bath is $\mu_o j^2$ where j is the current density and μ_o is permeability of free space. The average pinch force in the metal becomes $1/4\mu_o (j+jc)^2$ where jc is the vertical component of the current density vector on the bottom of the liquid metal. Assuming $j >> jc$, the difference in the pinch force becomes $3/4\ \mu_o j^2$ between in the bath and the metal. Assuming the movement of the interface surface is small compared to the ACD (anode-cathode distance) which is around 5 cm, the pinch force variation depending on the vertical movement of the interface surface is as follows:

$$3/2 \cdot \mu_o\, j^2/h_1 \cdot \zeta \qquad (\text{MKS unit}) \qquad (2)$$

where ζ is the displacement of the surface from its equilibrium position and h_1 is ACD. Thus, the motion equation for this wave becomes as follows:

$$(\rho_1/h_1 + \rho_2/h_2)\partial^2\zeta/\partial t^2 + 3/2 \cdot \mu_o\, j^2/h_1 \cdot \zeta = 0 \qquad (3)$$

h_1, h_2: ACD and the metal depth

This is a equation for a Harmonic oscillation where its angular velocity and period are expressed as follows:

$$\omega = \sqrt{3/2 \cdot \mu_o\, j^2/h_1 \;/\; (\rho_1/h_1 + \rho_2/h_2)} \simeq \sqrt{3/2 \cdot \mu_o/\rho_1} \cdot j \qquad (4)$$

$$T = 2\pi/\omega \qquad (5)$$

The dependency of the period on the current density was tabulated in Table 1.

local current density (amps/cm^2)	1	2	4	6	8	10
period (seconds)	20.9	10.5	5.2	3.5	2.6	2.1

Table 1. Short period wave

Thus, the intensity of the current is directly related to the period of this motion. The stronger the current concentration is, the shorter the period becomes.

Long Period Wave

This wave is essentially an internal gravity wave. The period of the wave can be calculated using a formula in classical fluid dynamics Eq.(5,7)[1]. The observations on this wave have been accumulated and reported since more than a decade ago [2,3,4,5,6]. In the aluminum reduction cell this wave is perturbed by the electromagnetic force (Lorentz force). This force varies along with the movement of the interface surface. Thus, the wave motion and the current distribution are described by a pair of coupled equations, one for the motion and another for the electrical potential distribution. This coupled equations were formulated by the author[1], as follows:

Wave Equation

$$(\rho_1/h_1 + \rho_2/h_2)\ \partial^2\zeta/\partial t^2 = \partial/\partial x \cdot \alpha\ \partial\zeta/\partial x + \partial/\partial y \cdot \alpha\ \partial\zeta/\partial y - j_y\ \partial B_z/\partial x + j_x\ \partial B_z/\partial y \qquad (6)$$

$$\alpha = g(\rho_2 - \rho_1)$$

Boundary Condition (rectangular shape)

$$\alpha\ \partial\zeta/\partial n = (n_x j_y - n_y j_x)\ B_z \qquad (7)$$

Equation for the electrical potential in the metal

$$\partial^2\phi/\partial x^2 + \partial^2\phi/\partial y^2 = -\ j/(h_1 h_2) \cdot \zeta \qquad (8)$$

$$j_x = -\ \partial\phi/\partial x,\quad j_y = -\ \partial\phi/\partial y$$

Boundary condition

$$\partial\phi/\partial n = 0 \qquad (9)$$

where x, y, z : cell length, width and depth direction
j_x, j_y : horizontal current density in the metal
B_z : vertical component of the magnetic flux density
n : unit normal vector on the boundary, outward positive
ϕ : electrical potential in the metal
j : current density in the bath

These coupled equations were solved using the Fourie series expansion and applied to the 140 kA side by side arrangement pot of the end risers and also to the 100 kA end to end arrangement pot[1]. A satisfactory agreement was obtained for both cases.

Application to the Kaiser 200 kA pot development

It is obvious from Equation (6) that the vertical magnetic field is a major source of perturbation. This vertical component also generates a convex interface surface in the

end riser pot by interacting with the horizontal current in the liquid metal. Thus, a practical requirement for the best bus arrangement is to reduce this vertical component.

Under this principle, a 200 kA cell magnetic field was designed neglecting analysis of the instability. The pot was constructed and operated since 1981 at Kaiser Tacoma plant[7]. Compared to a previous prototype end riser cell, operated from 1976 to 1979, the vertical component was reduced from 60 Gauss to 15 Gauss at its maximum value. Furthermore, the interface surface deformation, characteristic of KACC cells, was reduced from 12.5 cm to 2.5 cm.

To our disappointment, this newly constructed cell exhibited a long period wave (40 seconds period), and the cell was not as stable as we expected. So the instability analysis was undertaken. First, the interface wave was recorded using a computerized data acquisition system. A computer program was written to acquire the anode current distribution very rapidly and to calculate the interface displacement immediately so that the wave propagation could be observed on the site.

In parallel with the measurement, a mathematical treatment of the instability first made was to solve for the eigen value and eigen mode of the motion using the Fourie series analysis. The result plotted in Figure 1 is imaginary part of $(\rho_1/h_1+\rho_2/h_2)\omega^2$ as a function of the ACD for various Kaiser cells including the 200 kA cell. This revealed a stunning fact that the 200 kA cell was more unstable than the previous cell in which the magnetic field was 4 times larger and the interface displacement was over 10 cm.

The derivation of the instability was done in the following way. The Fourie series expansion for the solution turns the coupled equations into an eigen value problem for ω^2. This equation was solved using computer subroutine for eigen value for non-symmetric matrix. One eigen mode whose associated eigen value had an imaginary part was plotted in Figure 2. To confirm the result a computer simulation was made, which directly solved the coupled equations using finite difference method. The solution was compared to the results of the on-site measurements as shown in Figure 3. This comparison led to the following findings:

1. The larger interface surface movement at the upstream tap end corner was caused by the global distribution of the magnetic field over the interface surface. This movement was also badly amplified by the local distribution of the field at the corner.

2. Depending on the instability force, namely the linear growth rate of the wave, the wave sometimes takes quite a long time to fully develop itself. This explains that disturbances to the cell such as anode changeout,

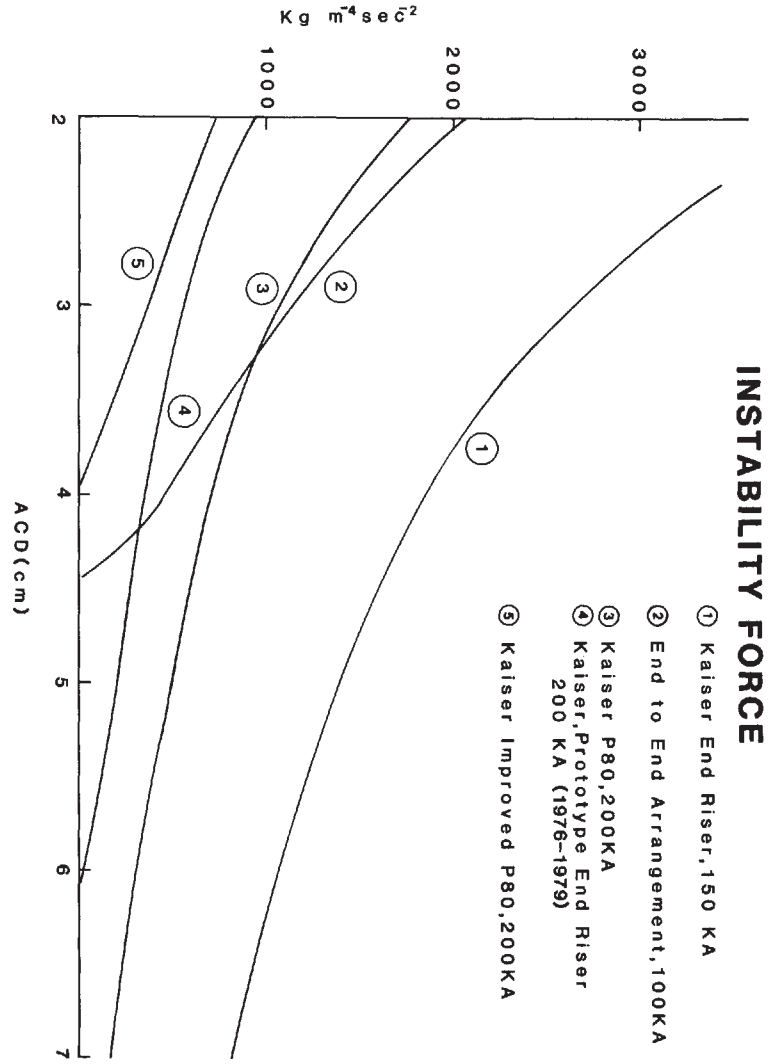

figure 1
INSTABILITY FORCE

figure 2
METAL PAD WAVE

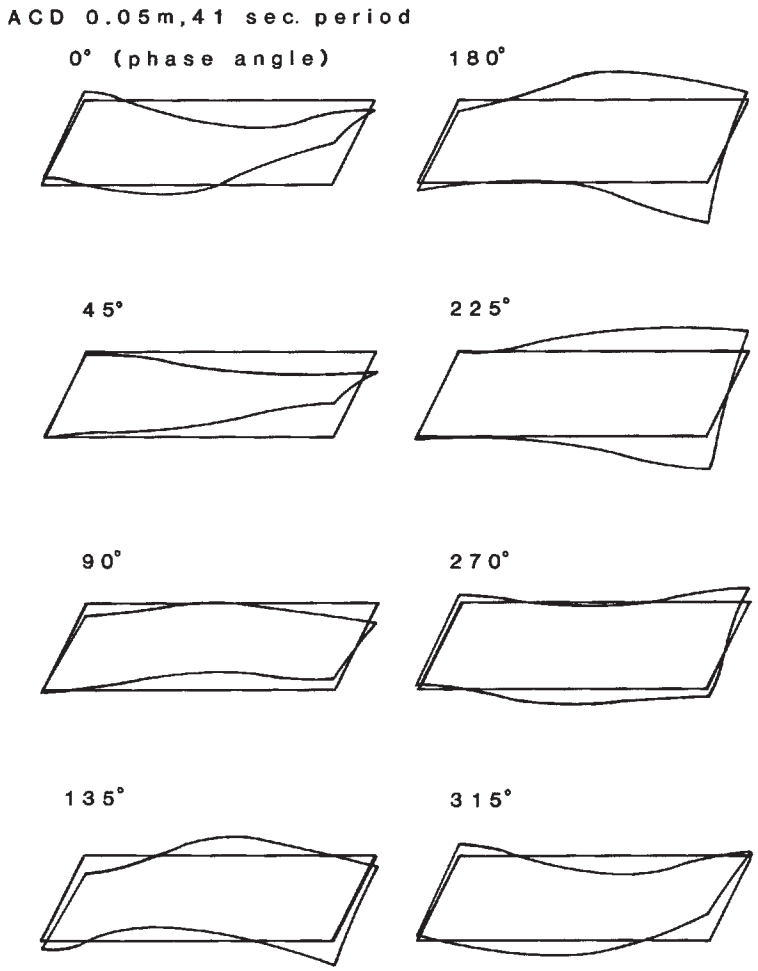

figure 3
METAL PAD WAVE COMPARISON

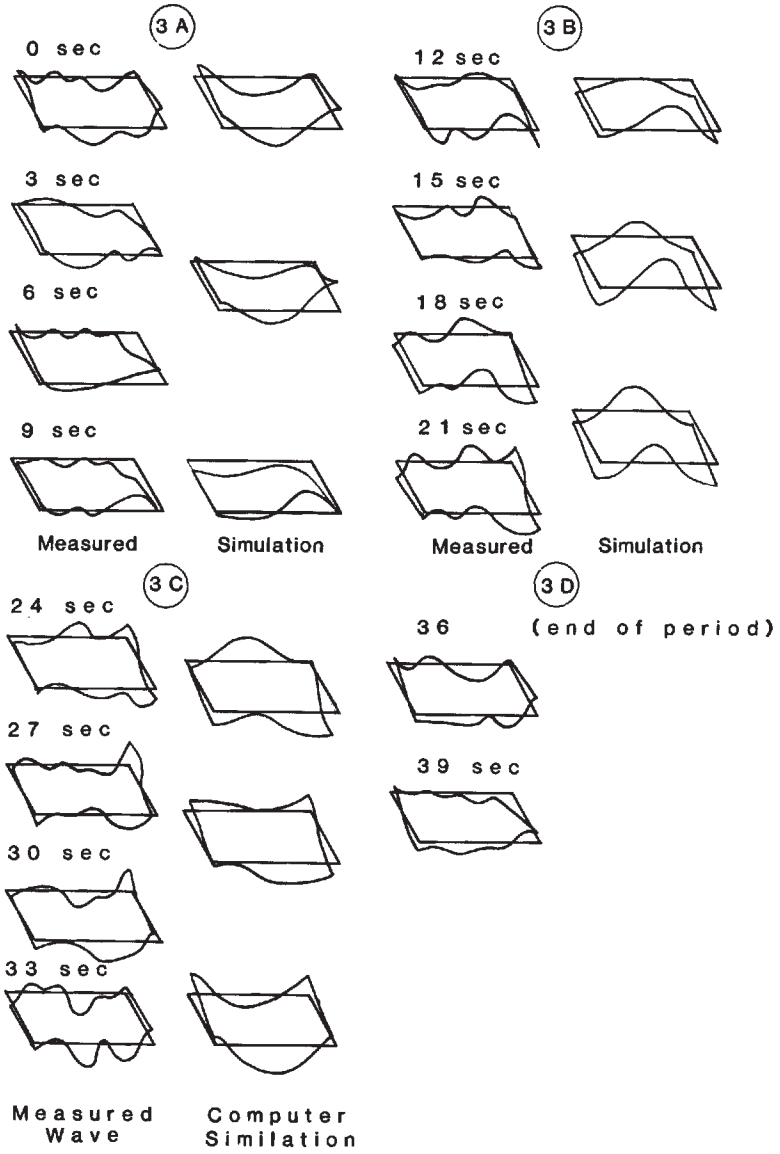

lowering the ACD or disturbance in feeding, results in palpable instability after hours.

Based on the evaluation of the instability the magnetic field was modified in such a way that the instability force is kept adequately low as shown in Figure 1. The voltage trace before and after the improvement is shown in Figure 4. The long period wave was effectively suppressed and scarcely observed. An improvement in current efficiency and pot voltage were 1.0% and 0.1 volts.

Conclusion

1. Pot instability can be evaluated quantitatively by solving a pair of the coupled partial differential equations. The linear growth rate for the wave determines the stability of the cell.

2. The magnetic field in our 200 kA prototype cell was modified based on this theory and as a result the pot instability was effectively reduced.

3. The distribution pattern of the magnetic field is rather more important than the maximum intensity of the field. In other words, a flatter metal pad does not always result in a higher stability because the flatness is a result of static balance and the instability is a matter of dynamics.

4. This fact indicates a possibility of increasing the pot stability in the existing reduction line without major alteration to the bus arrangement.

5. In the observation the short period wave was usually associated with the long period wave. A linear superposition of the two waves occurs in the cell.

6. The steel effect calculation is the most critical step in designing a magnetic field for a higher amperage cell. To achieve 10 Gauss field by cancelling the fields from two different conductors with their absolute intensities of order of 100 Gauss, the accuracy of the calculation should be ±10%. The steel effect calculation coded by the author relies on the dipole method presented by Sele[8]. Instead of using the rod element the plates were approximated with ellipsoids in our calculation.

After verification of the model with the measurements for various bus arrangements the steel shielding effect is now evaluated accurately without introducing a shielding factor which is essentially an adjustment factor. Thus, the elaborate instability analysis along with the accurate magnetic field calculation[7] made possible to pinpoint the problem,

figure 4
CELL VOLTAGE AND NOISE

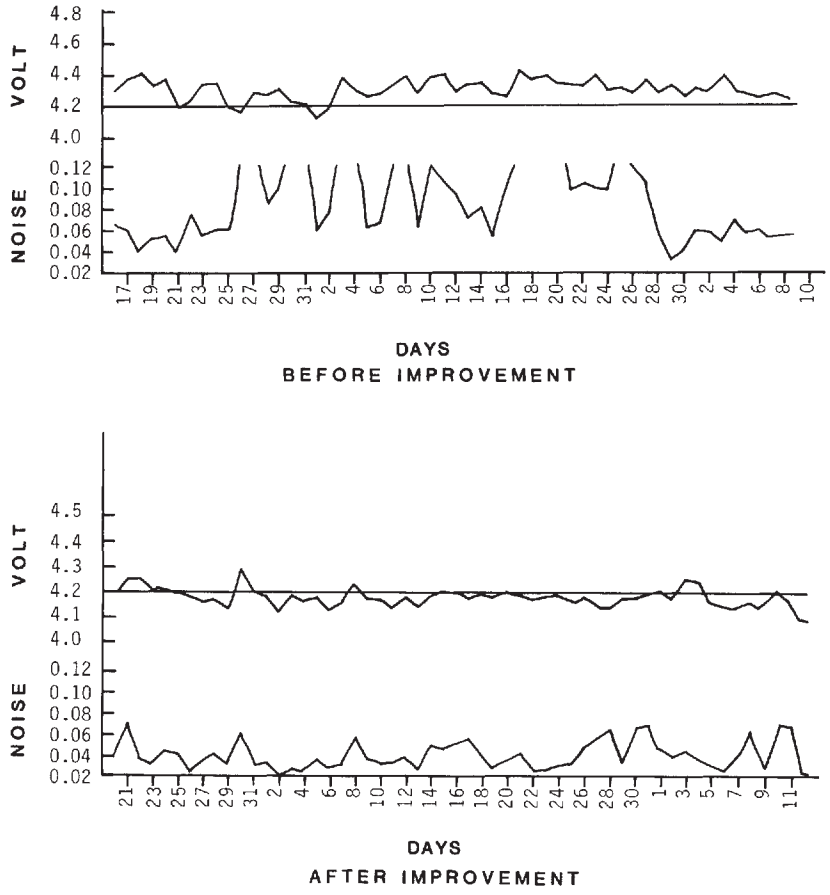

and led us to a prompt correction of it within one year after the cell start-up.

Acknowledgment

The author acknowledges all the members who joined the task force and performed the measurements.

References

1 N. Urata, K. Mori, and H. Ikeuchi, "Behavior of Bath and Molten Metal in Aluminum Electrolytic Cell," Kaikinzoku (Light Metals, Japan) Vol. 26, No. 11, 1976, pp. 573.

2 Schmitt-Hatting, "Investigations of Noise in Aluminum Electrolysis Cells," AIME Annual Meeting, New York, 1975.

3 K. Mori, K. Shiota, N. Urata, and H. Ikeuchi, "The Surface Oscillation of Liquid Metal in Aluminum Reduction Cells," Light Metals, Vol. 1, 1976, pp. 77.

4 S. Matsui and A. Era, "Measurement of Metal Imbalance in Aluminum Reduction Cell," Light Metals 1982, pp. 373.

5 S. Cherchi and G. Degan, "Oscillation of Liquid Aluminium in Industrial Reduction Cell," Light Metals 1983, pp. 457.

6 T. Sele, "Magnetic Fields, Flow, and Stability for Electrolytic Aluminum Reduction Cells," Paper Presented at ISE 30th Meeting, Tronheim, August 1979.

7 R. D. Zabreznik and E. D. Tarapore, "Development of the Kaiser Aluminum 195 kA Cell," Light Metals 1984, pp. 455.

8 T. Sele, "Computer Model for Magnetic Field in Electrolytic Cells, Including the Effects of Steel Parts," Light Metals 1973, pp. 119.